Bergische Universität Wuppertal

Fachbereich Mathematik und Naturwissenschaften

Institute of Mathematical Modelling, Analysis and Computational Mathematics
(IMACM)

Preprint BUW-IMACM 18/15

Piotr Putek, E. Jan W. ter Maten, Michael Günther, Andreas Bartel,

Shape optimization of a PM synchronous machine under probabilistic constraints

Oktober, 2018

Shape optimization of a PM synchronous machine under probabilistic constraints

Piotr Putek E. Jan W. ter Maten Michael Günther
Andreas Bartel

Bergische Universität Wuppertal, Gaußstraße 20, D-42119 Wuppertal, Germany

{putek,termaten,guenther,bartel}@math.uni-wuppertal.de

This paper proposes a robust and reliability-based shape optimization method to find the optimal design of a permanent magnet (PM) synchronous machine. Specifically, design of rotor poles and stator teeth is subjected to the shape optimization under manufacturing tolerances / imperfections and probabilistic constraints. In a forward problem, certain parameters are assumed to be random. This affects also a shape optimization problem, which is formulated in terms of a tracking-type robust cost functional and which is constrained by probabilistic constraints in order to attain a new, desired, robust design. The topological gradient is evaluated using the Asymptotic Expansion Method, to which we apply a Stochastic Collocation Method. In the end, to illustrate our approach, we provide the optimization results for a 2D model of the PM machine.

1 Introduction

Following with the rapid development of the performance of PM synchronous machines, they have been widely applied in various fields such as industrial automation, household applications and electric vehicles, etc. In particular, due to some advantages including high efficiency in the whole working region and a good dynamic performance, they have become the main type of a driving motor for electric vehicles [4].

Compared with the conventional surface-mounted PM synchronous machine, the ECPSM[1], on the one hand, has a wider speed range due to the field-weakening capability and better output torque characteristics [5]. On the other hand, it typically suffers from the considerable high level of a cogging torque (CT) because of its specific structure and a high air - gap flux density. This results in the undesired torque and speed ripples as well as acoustic noise and vibrations, that influence its further application.

[1] The Electrically Controlled Permanent Magnet Excited Synchronous Machine was investigated within the scientific project under grant no. N510 508040 (2011–2013), Poland.

Yet, as a result of manufacturing processes, a design of electric machines is strongly affected by the uncertainties in both the geometrical and material parameters [7]. Thus, to provide reliable simulations, a mathematical model with random input data needs to be considered [6]. This implies the use of the reliability analysis and the robust framework for a design assessment. The former allows for reducing the risk of a failure in an operating device and the latter results in minimizing the variability of the output performance functions.

In our paper, we formulate the shape optimization in terms of both concepts. Therefore, we combine the reliability-based and the robust approach for a design of the ECPSM in order to attain its new topology, that meets both considered criteria.

2 Forward problem with random input parameters

A mathematical model of the ECPSM [6] can be described by a quasilinear curl-curl equation with random input data $\mathbf{p}(\boldsymbol{\xi}) \in R^Q$, in a two dimensional setting $\mathbf{x} \in D \subset \mathbb{R}^2$ with Lipschitz boundaries $\partial D \in C^2$. Furthermore, let corresponding uncertainties be represented by certain random fields $\mathbf{p}(\boldsymbol{\xi}) \in R^Q$, where the random vector $\boldsymbol{\xi}$ is defined on a suitable probability space $(\mathscr{A}, \mathscr{F}, \mathbb{P})$ with an event space $\mathscr{A}$, a σ-algebra $\mathscr{F}$ and a probability measure $\mathbb{P}$. Then, for a magnetic vector potential $\mathbf{A} = (0,0,u)$ and $\chi := (\mathbf{x}, \boldsymbol{\xi}) \in D \times \Gamma_\rho$, the weak form reads as: find $u \in V_\rho$ such that

$$\left(\nu(|\nabla u(\chi)|^2)\nabla u(\chi), \nabla \varphi(\chi)\right) = (f, \varphi(\chi)) \tag{1}$$

for all $\varphi \in V_\rho$ with $V_\rho = L^2\left(H_0^1(D)\right) \otimes L_\rho^2\left(\Gamma_\rho\right)$ and its corresponding norm $\|u\|_{V_\rho}^2 = (u,u) := \int_{\mathrm{D}} \mathbb{E}\left[|\nabla u|^2\right] d\boldsymbol{x}$, where $\mathbb{E}(\cdot)$ denotes the expectation value for $\mathbb{P}$. The function f is defined by $f(\chi) = J_i(\chi) + \nu_{\mathrm{PM}}(\chi)\nabla \cdot \mathbf{M}(\chi)$, where J_i, $\mathbf{M}(\chi)$ and $\nu_{\mathrm{PM}}(\chi)$ denote the current density, the magnetization and the reluctivity of the PM, respectively.

Stochastic Model for Material Parameters. Due to the uncertainty of some parameters associated with the presented model (1), which are therefore modeled as random variables, we proceed with further uncertainty inclusion. Here, a reluctivity model including the soft iron material $\nu(\mathbf{x}) : D \times \mathbb{R}_0^+ \rightarrow \mathbb{R}^+$ is assumed, as in [1], to be monotone, bounded and differentiable with a well-defined derivative satisfying $\alpha \leq \partial_B \nu \leq \gamma$ with $B = |\nabla u|$. Thus, its stochastic counterpart is given by

$$\nu(\chi) = \begin{cases} \nu_{\mathrm{Fe}}(\mathbf{x}, |\nabla u(\chi)|^2)\,[1 + \delta_1 \Upsilon(\xi_1)] & \text{for } \mathbf{x} \in D_{\mathrm{rot}}, \\ \nu_{\mathrm{Fe}}(\mathbf{x}, |\nabla u(\chi)|^2)\,[1 + \delta_2 \Upsilon(\xi_2)] & \text{for } \mathbf{x} \in D_{\mathrm{sta}}, \\ \nu_0(\mathbf{x})\,[1 + \delta_3 \Upsilon(\xi_3)] & \text{for } \mathbf{x} \in D_{\mathrm{air}}, \\ \nu_{\mathrm{PM}}(\mathbf{x})\,[1 + \delta_4 \Upsilon(\xi_4)] & \text{for } \mathbf{x} \in D_{\mathrm{PM}}, \end{cases} \tag{2}$$

with vaccum reluctivity ν_0 and the domain $D = D_{\mathrm{air}} \cup D_{\mathrm{PM}} \cup D_{\mathrm{rot}} \cup D_{\mathrm{sta}}$ consisting of the area of air, the region of the PM and the iron domain for a rotor and a stator, respectively. We also consider $\mathbf{M}(\chi) = b_r\,[1 + \delta_5 \Upsilon(\xi_5)]\,\mathbf{T}(\mathbf{x})$, where b_r is the remanence flux density and $\mathbf{T}(\mathbf{x})$ denotes the magnetization direction. The mean values are denoted by δ_i, $i = 1, \ldots, 4$ and $\boldsymbol{\xi} = (\xi_1, \ldots, \xi_5)$ are the Gaussian random variables and $\Upsilon(\cdot) := \arctan(\cdot)$ is a normalized nonlinear function used due to the infinite support of the Gaussian distribution-function.

3 Reliability and Robustness Analysis

To assess the reliability and robustness of the electric machine design w.r.t uncertain input parameters arisen from, e.g., manufacturability, we explore the stochastic collocation method (SCM) compound with the polynomial chaos expansion (PCE).

3.1 The pseudo-spectral approach

For the the uncertainty quantification (UQ), we used the spectral approach by [9], where the quantities of interests to be calculated are the unknown expansion coefficient of the polynomial chaos.

Random Input Discretisation. As usually [10], a probabilistic modeling of uncertainties is applied to parametrize the probability triple. Within this approach, a random field is modeled by an univariate random vector with independent components and a known probability law $\mathbb{P}$. Hence, we define a vector with Gaussian random parameters as $\mathbf{p}(\boldsymbol{\xi}) = (p_1(\xi_1),\dots,p_Q(\xi_Q)) \in \mathbb{R}^Q$. Furthermore, denote by $\Gamma_q \equiv p_q(\mathscr{A}) \in \mathbb{R}$ the image of p_q with its support $\Gamma_\rho = \prod_{q=1}^{Q} \Gamma_q \subset \mathbb{R}^Q$ and let the $\rho_q :\ \Gamma_q \to \mathbb{R}^+$ be the probability density function (PDF) of the random variable $p_q(\xi),\ \xi \in \mathscr{A}$, for $q = 1,\dots,Q$. Then, we assume that a joint PDF of the independent random variables $\mathbf{p}(\boldsymbol{\xi})$ exist and is given by

$$\rho(\mathbf{p}) = \prod_{q=1}^{Q} \rho_q(p_q). \tag{3}$$

As a result, it allows to proceed with numerical calculations in the space $(\Gamma_\rho, \mathscr{B}^q, \rho d\mathbb{P})$ with Γ_ρ the image of the joint probabilistic density function ρ, $\mathscr{B}^q$ the q-dimensional Borel space and $\rho d\mathbb{P}$ a probabilistic measure, respectively.

Polynomial Chaos within the SCM. Later on, we consider the probabilistic Hilbert space $L^2_\rho(\Gamma_\rho) = \{Y(\mathbf{p}) : \mathbb{E}[Y(\mathbf{p})^2] < \infty\}$ equipped with a norm $\|Y\|^2_{L^2_\rho} = \langle Y,Y\rangle_\rho$, where we define the expected value of a random function $Y(\mathbf{p}) : \Gamma_\rho \to \mathbb{R}$ and an inner product for two random functions $Y(\mathbf{p}), Z(\mathbf{p}) : \Gamma_\rho \to \mathbb{R}$ by

$$\mathbb{E}[Y(\mathbf{p}(\boldsymbol{\xi}))] := \int_{\Gamma_\rho} Y(\mathbf{p})\rho(\mathbf{p})\,\mathrm{d}\mathbf{p}, \quad \langle Y(\mathbf{p}), Z(\mathbf{p})\rangle_\rho := \mathbb{E}(Y(\mathbf{p})Z(\mathbf{p})). \tag{4}$$

Consequently, the variance of a random function $Y(\mathbf{p}) \in L^2_\rho(\Gamma_\rho)$ read as

$$\mathrm{Var}[Y(\mathbf{p})] := \mathbb{E}[Y(\mathbf{p})^2] - \mathbb{E}[Y(\mathbf{p})]^2. \tag{5}$$

Now, to provide the spectral expansion of stochastic processes, for a function $u \in L^2_\rho(\Gamma_\rho)$, we introduce a truncated PC expansion [10]

$$\widetilde{u}(\boldsymbol{x},\mathbf{p}) \doteq \sum_{m=0}^{M} u_m(\boldsymbol{x})\,\Phi_m(\mathbf{p}) \tag{6}$$

with a complete set of multivariate polynomials $\Phi_m : \mathbb{R}^Q \to \mathbb{R}$, whose bases correspond to the PDF used for the description of input random parameters, that is, the uniform distribution implies the Legendre polynomials, while the Hermite polynomials refers to the Gaussian-type PDF, respectively.

In equation (6), u_m are *a priori* unknown coefficient functions to be determined by using projections of provided solutions at quadrature points on the basis polynomials as

$$u_m(\boldsymbol{x}) = \langle \widetilde{u}(\boldsymbol{x},\mathbf{p}), \Phi_m(\mathbf{p})\rangle_\rho . \tag{7}$$

Next, to approximate the probabilistic integrals of (7), we applied the Stroud formulas with a constant weight function [9] in the form

$$u_m(\boldsymbol{x}) \doteq \sum_{k=1}^{K} w_k \, \widetilde{u}\left(\boldsymbol{x},\mathbf{p}^{(k)}\right) \Phi_m\left(\mathbf{p}^{(k)}\right), \tag{8}$$

in which the w_k and $\mathbf{p}^{(k)}$ are deterministic quadrature weights and points. This type of quadrature methods is exact for multivariate polynomials up to the degree d_{PC}, *e.g.*, $K = 2Q$ for $d_{\mathrm{PC}} = 3$ and $K = 2Q^2+1$ for $d_{\mathrm{PC}} = 5$. They seem to be highly efficient especially in high-dimensional spaces ($Q \gg 1$) [6, 10], but their accuracy, unfortunately, is fixed and cannot be improved. Finally, the statistical moments are approximated by (including quadrature)

$$\mathbb{E}\left[\widetilde{u}(\boldsymbol{x},\mathbf{p})\right] \doteq u_0(\boldsymbol{x}), \quad \mathrm{Var}\left[\widetilde{u}(\boldsymbol{x},\mathbf{p})\right] \doteq \sum_{m=1}^{M} |u_m(\boldsymbol{x})|^2, \tag{9}$$

using $\Phi_0 = 1$ [9]. In addition, other quantities such as the local sensitivity and the variance-based global sensitivity can easily be calculated based on (6) as well [8, 10].

3.2 Reliability index approach

We use the First-Order Reliability Method (FORM) [11] to evaluate the reliability criteria. After transforming the selected random variables $\mathbf{r} \subset \mathbf{p}$ into the standard normal space by $\boldsymbol{\xi}_r = \mathbf{T}_{\xi_r}(\mathbf{r})$, the reliability index β is found by solving the constraint optimization problem (excluding a trivial case $\boldsymbol{\xi}_r = 0$)

$$\begin{aligned} \beta^* = \min_{\boldsymbol{\xi}_r} \quad & \beta(\boldsymbol{\xi}_r) = \sqrt{(\boldsymbol{\xi}_r{}^\top \boldsymbol{\xi}_r)} \\ \text{s.t.} \quad & g(\boldsymbol{\xi}_r, \cdot) = 0, \end{aligned} \tag{10}$$

where $g(\boldsymbol{\xi}_r,\cdot)$ is a limit state function. The failure probability is approximated by $\mathbb{P}[g(\Omega,u(\cdot)) \leq 0] \approx \Phi(-\beta^*)$, where $\Phi(\cdot)$ is the standard normal cumulative distribution function. Consequently, the resulting normalized vector $\boldsymbol{\xi}_r^*$ is used to modify the random vector $\mathbf{r}^*$, which influences the UQ of a model (1).

4 Shape Optimization Problem

For this reason, we consider a cost functional, defined in terms of the magnetic energy [5] as

$$F(\Omega, u(\chi)) = \frac{1}{2}\int_D \nu |\nabla u(\chi)|^2 d\mathbf{x} \tag{11}$$

with $\Omega = D_{\text{rot}} \cup D_{\text{sta}} \cup D_{\text{PM}}$. Thus, the shape optimization problem is given by

$$\inf_{\Omega} \mathscr{E}\left[F\left(\Omega, \widetilde{u}(\mathbf{p})\right)\right] := \mathbb{E}\big[F\left(\Omega, u(\cdot)\right)\big] + \iota\sqrt{\operatorname{Var}\big[F\left(\Omega, u(\cdot)\right)\big]} \tag{12a}$$

$$\text{s.t.} \quad \beta(\cdot) \geq \beta_t, \tag{12b}$$

$$u \text{ satisfies } (1), \tag{12c}$$

with the prescribed parameters $\iota = 6$ and $\beta_t = 3.8$, where the probabilistic constraint (12b) was expressed by an equivalent form using the reliability index approach (10). For the solution of the problem (12a)–(12c), we construct an iterative scheme [6], which requires developing a topological derivative.

Topological Derivative for the Fixed Cubature Point. Given the result in [2], upgraded by the respective magnetization and the excitation terms $\nu_{\text{PM}}\mathbf{M}$ and $J_i(\mathbf{x})$, respectively, the topological derivative, calculated at the fixed k-th quadrature point, i.e., $u^{(k)}(\mathbf{p}^{(k)}) =: u$, is defined by

$$\begin{aligned} F\left(\Omega_\varepsilon, \cdot\right) - F\left(\Omega, \cdot\right) &\doteq \varepsilon^2[\nu_0^+ - \nu^-(|\nabla u(\mathbf{x}_0)|^2)][\nabla u(\mathbf{x}_0)\mathscr{P}\left(\vartheta_a, \nu^+, \nu^-, u(\mathbf{x}_0)\right)\nabla\lambda(\mathbf{x}_0)] \\ &+ \varepsilon^2[\nu_0^+ - \nu_{\text{PM}}^-][\nabla u(\mathbf{x}_0)\mathscr{P}\left(\vartheta_a, \frac{\nu_0^+}{\nu_{\text{PM}}^-}\right)\nabla\lambda(\mathbf{x}_0)] + 4\pi\varepsilon^2[\mathbf{M}^+(\mathbf{x}_0) - \mathbf{M}^-(\mathbf{x}_0)]\nabla\lambda(\mathbf{x}_0) \\ &+ \varepsilon^2 2\pi[J^+(\mathbf{x}_0) - J^-(\mathbf{x}_0)]\lambda(\mathbf{x}_0), \end{aligned} \tag{13}$$

where the perturbed domain Ω_ε is defined in $\omega_\varepsilon := \boldsymbol{x}_0 + \varepsilon\vartheta_a$, where ϑ_a is an ellipse or the unit disc, ε denotes the perturbation parameter and $\mathscr{P}(\cdot)$ is the polarization matrix. For details we refer to [2]. Moreover, to accelerate the topological derivative calculation, a dual problem for $F^{(k)}(\Omega, u^{(k)})$ with an adjoint variable $\lambda^{(k)} =: \lambda$ is defined as

$$a(\lambda, \psi) = (dF[\Omega, u], \psi),$$

in which the bilinear form $a(\lambda, \psi) := \big(\nu(|\nabla u(\mathbf{x})|^2)\nabla u(\mathbf{x}), \nabla\psi(\mathbf{x})\big)$.

Topological Derivative for the Robust Functional. Furthermore, when the SCM with PCE is involved in the optimization procedure, we can use (6) to represent the functional $F^{(k)}$ as in (11) and also the topological derivative $dF^{(k)}$ as in (13) as the truncated response surface models

$$\widetilde{F}(\boldsymbol{x}, \mathbf{p}) \doteq \sum_{m=0}^{M} F_m(\boldsymbol{x})\Phi_m(\mathbf{p}), \qquad d\widetilde{F}(\boldsymbol{x}, \mathbf{p}) \doteq \sum_{m=0}^{M} dF_m(\boldsymbol{x})\Phi_m(\mathbf{p}). \tag{14}$$

Next, to obtain the unknown expansion coefficient $F_m(\boldsymbol{x})$ and $dF_m(\boldsymbol{x})$, the provided solutions $F^{(k)}$ and $dF^{(k)}$ at the corresponding quadrature point $k = 1, \ldots, K$ is projected into the polynomial basis using (8). Then, the *robust* topological derivative of the expectation value and of the variance are given by

$$d\,\mathbb{E}[F(\Omega, \widetilde{u}(\mathbf{p}))] = dF_0(\boldsymbol{x}), \qquad d\operatorname{Var}[F(\Omega, \widetilde{u}(\mathbf{p}))] = \sum_{m=1}^{M} 2F_m(\boldsymbol{x})\,dF_m(\boldsymbol{x}). \tag{15}$$

To the end, the topological derivative of the robust functional (12a) reads as

$$d\mathscr{E}\left[F\left(\Omega,\widetilde{u}(\mathbf{p})\right)\right] = d\mathbb{E}\left[F\left(\cdot\right)\right] + 0.5\,\iota\left(\sqrt{\mathrm{Var}\left[F\left(\cdot\right)\right]}\right)^{-1} d\,\mathrm{Var}\left[F\left(\cdot\right)\right], \tag{16}$$

where the mean and the variance are approximated by

$$\mathbb{E}\left[F\left(\Omega,\widetilde{u}(\mathbf{p})\right)\right] = F_0(\boldsymbol{x}), \qquad \mathrm{Var}\left[F\left(\Omega,\widetilde{u}(\mathbf{p})\right)\right] = \sum_{m=1}^{M} F_m^2\left(\boldsymbol{x}\right). \tag{17}$$

Optimization Procedure for the Reliability Index. To solve the invariant problem (10), we use the iteration procedure,in which a design point is defined as $\boldsymbol{\xi}_r = \beta\cdot\boldsymbol{\alpha}$. Therein, the normal vector to the function g, i.e, a gradient for $i,j = 1,\ldots,N$ takes the form

$$\alpha_i = -\partial_{\xi_{r_i}} g\left(\beta\cdot\alpha\right)\cdot\left(\sum_{j=1}^{N}\left[\partial_{\xi_{r_j}} g\left(\beta\cdot\alpha\right)\right]^2\right)^{-1/2}.$$

Finally, the reliability index is defined as $g(\beta\cdot\alpha_1,\ldots,\beta\cdot\alpha_J) = 0$.

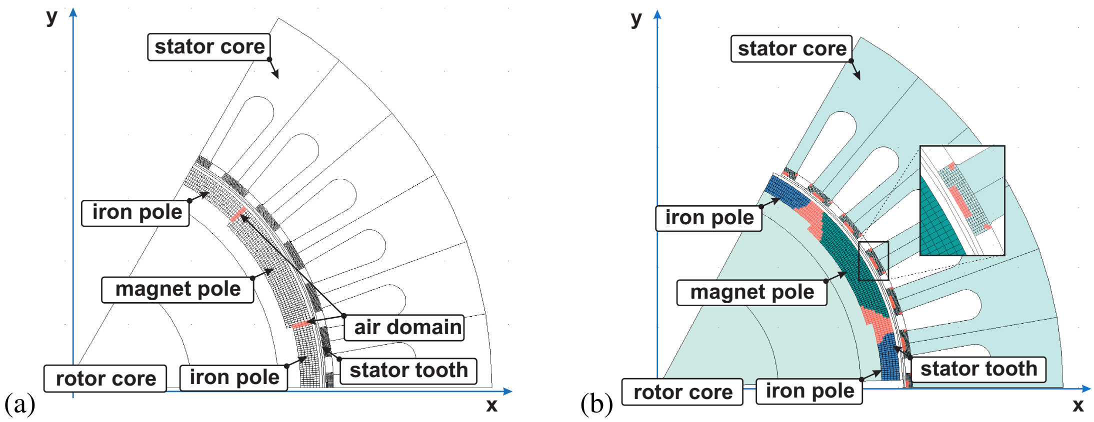

Figure 1: ECPSM topology before and after optimization: (a) an initial model, (b) the optimized configuration found at 15^{th} iteration.

Implementation Remarks. In practical implementation, first, we expand a function $g(\cdot)$, e.g., the air-gap magnetic flux density (MFD), in the form of a surface model using (6). Secondly, the global sensitivity analysis [8] can be used to identify the most influential input parameters w.r.t the variation of the function g. Then, we solve an invariant problem (10) in order to find the reliability index β. Next, based on the local sensitivity analysis [10] (a sign of mean values derivative w.r.t the particular random input variables), $\mathbf{p}(\boldsymbol{\xi})$ = [$\nu_{\mathrm{Fe}}^{\mathrm{sta}}(\xi_1)$, $\nu_{\mathrm{Fe}}^{\mathrm{rot}}(\xi_2)$, $\nu_{\mathrm{air}}(\xi_3)$, $\nu_{\mathrm{PM}}^{*}(\xi_4)$, $b_r^{*}(\xi_5)$] is modified using $\boldsymbol{\xi}$ as in (2). To the end, this algorithm can be incorporated into the sensitivity-based optimization flow in order to find the robust and reliable low cogging design of the ECPSM. Likewise, to the reliability-based topology method [3], this procedure does not contain the nested robust and reliability loops.

5 Numerical example and discussion

We used the proposed method to design the rotor poles as well as the base tooth in the stator of the ECPSM machine at on-load condition, i.e., the model of the ECPSM was supplied with $I_n = 15[A]$, $n = 1,2,3$. The 2D finite elements model, which consisted of a triangular mesh with the second order Lagrange polynomials, for the A-potential formulation was built in the COMSOL 3.5a. The sensitivity-based algorithm for the topology optimization was implemented in MATLAB 7.10. The area of rotor in the initial 2D model was divided into 360 and 480 voxels for the iron and the PM poles, while the base teeth was composed of 512 voxels. For simplicity, in our work we considered as the limit state function $f_{\mathrm{PM}}(\chi) = \int_D \nu_{\mathrm{PM}}(\chi)\nabla\cdot\mathbf{M}(\chi)d\boldsymbol{x} =: g(\chi)$with $\beta_t = 3.8$, which corresponds to the the (Gaussian) failure probability $P_f = 10^{-4}$. Here, scalings in (2) are $\delta_{1-4} = 0.15$ and $\delta_5 = 0.1$. Additionally, in the postprocesing stage, the ECPSM was analyzed in the magnetoquasistatic regime with $\sigma_{\mathrm{FE}} = 11.2\,\mathrm{M}\,[S/m]$ in order to investigate the core losses, shown on Fig.3 (b).

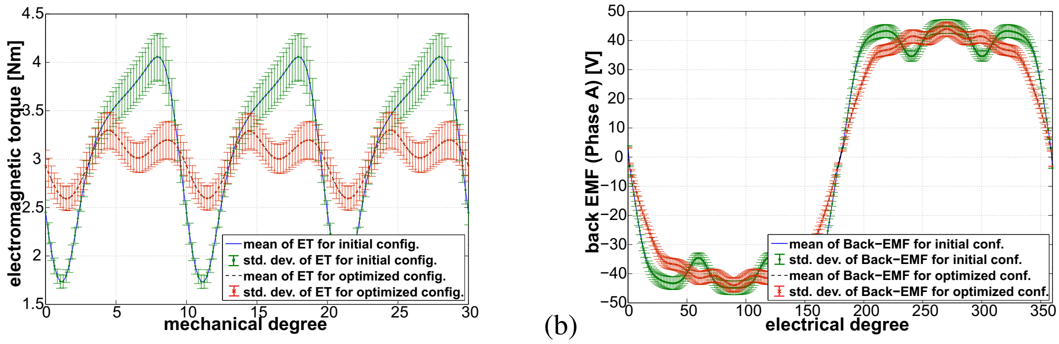

(a) (b)

Figure 2: Statistical moments for electromagnetc torque (ET) and back electromotive force (EMF).

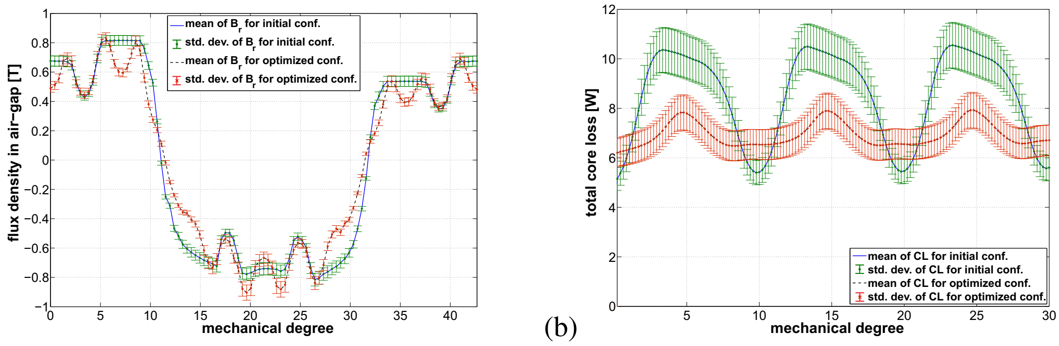

(a) (b)

Figure 3: Statistical moments for the MFD in the air-gap and the core losses (CL).

6 Conlusions

We demonstrated how to efficiently incorporate the reliability analysis into the robust framework to accomplish such a design of the ECPSM, depicted in Fig. 1, which is not only resistant to input variations, but also satisfies safety criteria. The mean value and the standard deviation of both the ET and the back EMF are depicted on Figs. 2. We could observe a decrease of statistical moments for both considered quantities by $5\%/7\%$ and $21\%/23\%$, respectively. These results extend our outcomes provided in [6].

References

[1] I. Cimrák. Material and shape derivative method for quasi-linear elliptic systems with applications in inverse electromagnetic interface problems, 2012.

[2] P. Gangl, S. Amstutz, and U. Langer. Topology optimization of electric motor using topological derivative for nonlinear magnetostatics. *IEEE Trans. on Magn.*, 52(3):1–4, March 2016.

[3] G. Kharmanda, N. Olhoff, A. Mohamed, and M. Lemaire. Reliability-based topology optimization. *Struct. Multidisc. Optim.*, 26(5):295–307, 2004.

[4] S. Morimoto, Y. Asano, T. Kosaka, and Y. Enomoto. Recent technical trends in PMSM. In *2014 IPEC-Hiroshima 2014 - ECCE ASIA*, pages 1997–2003, May 2014.

[5] P. Putek. Nonlinear magnetoquasistatic interface problem in a PM machine with stochastic PDE constraints. *accepted for the publication in the Engineering Optimization*, September 2017.

[6] P. Putek, E.J.W. ter Maten, M. Günther, and J.K. Sykulski. Variance-based robust optimization of a permanent magnet synchronous machine. *IEEE Trans. on Magn.*, 54(3):1–4, 2018.

[7] P. Sergeant, G. Crevecoeur, L. Dupré, and A. Van den Bossche. Characterization and optimization of a permanent magnet synchronous machine. *COMPEL*, 28(2):272–285, 2009.

[8] B. Sudret. Global sensitivity analysis using polynomial chaos expansions. *Reliab. Eng. & Sys. Safety*, 93(7):964 – 979, 2008.

[9] D. Xiu. Efficient collocational approach for parametric uncertainty analysis. *Commun. Comput. Phys.*, 2(2):293–309, 4 2007.

[10] D. Xiu. *Numerical methods for stochastic computations: A spectral method approach*. Princeton University Press, United States, 7 2010.

[11] Y.G. Zhao and T. Ono. A general procedure for first/second-order reliability method (FORM/SORM). *Structural Safety*, 21(2):95 – 112, 1999.